Available online at www.sciencedirect.com
SCIENCE DIRECT®
Journal of Computational Physics 188 (2003) 123–138
JOURNAL OF COMPUTATIONAL PHYSICS
www.elsevier.com/locate/jcp

A Coulomb collision model for PIC plasma simulation

David J. Larson *

Lawrence Livermore National Laboratory, University of California, Livermore, CA 94550, USA

Received 4 September 2002; received in revised form 19 February 2003; accepted 20 February 2003

Abstract

A new approach to modeling partially collisional plasmas that provides a smooth transition from the fluid (Coulomb collision dominated) to the fully kinetic PIC (collisionless) limit is presented. In addition to the usual quantities of mass, charge, and velocity, each particle carries an isotropic Maxwellian velocity distribution. Higher resolution of velocity space is achieved by generating more particles using a procedure that preserves the first four velocity moments. This velocity space fragmentation is essential for capturing non-Maxwellian plasma behavior. The model developed here allows the efficient simulation of partially collisional plasmas by reducing both the number of particle pairings required per time step and the number of particles needed to retain non-Maxwellian plasma behavior. The method produces reasonable results when the time step is large relative to the collision frequencies and works in the limit of one particle per species per cell. Particle merging can be exploited to control the number of particles in a natural way. The collision process is fully three-dimensional and conserves energy and momentum exactly. Results from 3v and 1d3v simulations are presented and compared with previous multi-fluid and fully kinetic PIC simulations.

1. Introduction

Particle-in-cell (PIC) codes are an effective tool for modeling collisionless plasmas. For collisional plasmas, the most widely used approach is to model the plasma as a fluid. The intermediate regime, sometimes referred to as "partially collisional", is less thoroughly explored.

Takizuka and Abe [1] developed a binary Monte-Carlo collision model for equally weighted simulation particles that remains the standard approach. The model requires pairing all the particles in a cell randomly by species (ion–ion, ion–electron, electron–electron) and colliding particle pairs. The variable $\delta = \tan(\Theta/2)$, where Θ is the scattering angle in the relative velocity frame, is chosen randomly from a Gaussian distribution with zero mean and variance given by

$$\langle \delta^2 \rangle = \frac{Z_\alpha Z_\beta e^4 n_L \lambda}{8\pi\varepsilon_0^2 m_{\alpha\beta}^2 u^3}\Delta t, \tag{1}$$

* Tel.: +1-925-423-9323; fax: +1-925-423-9208.
E-mail address: larson6@llnl.gov (D.J. Larson).

0021-9991/03/$ - see front matter © 2003 Elsevier Science B.V. All rights reserved.
doi:10.1016/S0021-9991(03)00157-8

where ε_0 is the vacuum permittivity, n_L is the lower of n_α and n_β, and λ is the Coulomb logarithm. Although it is computationally intensive, the model conserves total momentum and energy and describes a collision integral of the Landau form.

Jones et al. [2] present an algorithm for modeling partially collisional plasmas using a grid-based "collision field" for interspecies collisions. This collision field is incorporated into the Lorentz force equation when the particle velocities are updated. For intra-species collisions an approach based on the Langevin equation is used. The collision frequencies employed are those derived by Decoster from a rigorous analysis of the fluid transport equations derived from the Boltzmann equation for two or more species. Two collision frequencies are defined, one associated with dynamic friction and the other related to temperature equilibration. While promising, there are several known problems with the Jones approach. In the cold beam limit (thermal velocity small compared to the relative drift velocity) the intra-species algorithm slowing down rate exceeds the Fokker–Planck value with a minimum over-prediction of 3.8. The interspecies algorithm also yields incorrect results if the distributions are far from Maxwellian [3].

Miller and Combi [4] extend Takizuma and Abe's binary collison algorithm to particles with unequal weights by introducing a weighting factor for each pair-wise interaction. An important feature of their algorithm is that the particles within a cell are randomly paired only once each time step. Charged particles within a given spatial grid cell are pair-wise scattered, explicity conserving momentum and implicitly conserving energy.

In this paper I present a Coulomb collision algorithm for PIC plasma simulation based on the interaction of particles carrying isotropic Maxwellian velocity distributions. Higher resolution of velocity space is achieved by fragmenting the velocity distribution in order to produce more particles. Post-collision merging can be employed to reduce the number of simulation particles in a natural way. The fragmentation procedure preserves the first four moments of the original velocity distribution. Higher moments could be used to further constrain the fragmentation procedure; however, little benefit would result given the very small error introduced using the procedure described below. Varying the amount of fragmentation allows a smooth transition between results obtained via a multi-fluid algorithm and those obtained by a fully kinetic Monte-Carlo collision algorithm.

2. Velocity distribution fragmentation

In addition to the usual quantities of mass, charge, and drift velocity, each simulation particle carries an isotropic Maxwellian velocity distribution. Each simulation particle has the following velocity distribution:

$$\frac{W_0}{(2\pi)^{3/2} v_{\mathrm{th}}^2} \exp\left[-\frac{(\vec{v} - \vec{u}_0)^2}{2 v_{\mathrm{th}}^2} \right], \tag{2}$$

where the thermal velocity $v_{\mathrm{th}} = \sqrt{k_{\mathrm{B}} T / m}$, the particle drift velocity is $\vec{u}_0$, and the numerical weight of the particle is W_0.

In order to capture velocity-dependent features of the plasma, the velocity distribution function may be fragmented in order to produce more simulation particles, as described by Hewett [6]. Although similar, the following procedure uses the fourth moment instead of the one-sided momentum employed by Hewett. Consider splitting just the x component of velocity into three pieces. Each piece is a new particle, so in place of one original particle located at x_0 we generate three new particles all located at x_0. The weight and thermal velocity of the new particles are less than those of the original particle. Fig. 3 illustrates the fragmentation procedure with the original one particle distribution shown by the solid line and the three new particle distributions plotted with dotted lines.

The 0th, 2nd, and 4th moments of the velocity distribution are used to define a unique splitting in velocity space. The moment equations yield

$$w_0 = w_\mathrm{m} + 2w_\mathrm{p}, \tag{3}$$

$$\left(u_{x0}^2 + v_{\mathrm{th}x0}^2 + v_{\mathrm{th}y0}^2 + v_{\mathrm{th}z0}^2\right)w_0 = \left(u_{x0}^2 + v_{\mathrm{th}x\mathrm{m}}^2 + v_{\mathrm{th}y0}^2 + v_{\mathrm{th}z0}^2\right)w_\mathrm{m} + \left((u_{x0} - u_{x\mathrm{p}})^2 + v_{\mathrm{th}x\mathrm{p}}^2 + v_{\mathrm{th}y0}^2 + v_{\mathrm{th}z0}^2\right)w_\mathrm{p} + \left((u_{x0} + u_{x\mathrm{p}})^2 + v_{\mathrm{th}x\mathrm{p}}^2 + v_{\mathrm{th}y0}^2 + v_{\mathrm{th}z0}^2\right)w_\mathrm{p}, \tag{4}$$

$$\begin{aligned}&\left(u_{x0}^4 + 2v_{\mathrm{th}x0}^2v_{\mathrm{th}y0}^2 + 2v_{\mathrm{th}x0}^2v_{\mathrm{th}z0}^2 + 3v_{\mathrm{th}x0}^4 + 2u_{x0}^2\left(3v_{\mathrm{th}x0}^2 + v_{\mathrm{th}y0}^2 + v_{\mathrm{th}z0}^2\right)\right)w_0\\ &\quad= \left(u_{x0}^4 + 2v_{\mathrm{th}x\mathrm{m}}^2v_{\mathrm{th}y0}^2 + 2v_{\mathrm{th}x\mathrm{m}}^2v_{\mathrm{th}z0}^2 + 3v_{\mathrm{th}x\mathrm{m}}^4 + 2u_{x0}^2\left(3v_{\mathrm{th}x\mathrm{m}}^2 + v_{\mathrm{th}y0}^2 + v_{\mathrm{th}z0}^2\right)\right)w_\mathrm{m} + \left((u_{x0} - u_{x\mathrm{p}})^4\right.\\ &\qquad\left. + 2v_{\mathrm{th}x\mathrm{p}}^2v_{\mathrm{th}y0}^2 + 2v_{\mathrm{th}x\mathrm{p}}^2v_{\mathrm{th}z0}^2 + 3v_{\mathrm{th}x\mathrm{p}}^4 + 2(u_{x0} - u_{x\mathrm{p}})^2\left(3v_{\mathrm{th}x\mathrm{p}}^2 + v_{\mathrm{th}y0}^2 + v_{\mathrm{th}z0}^2\right)\right)w_\mathrm{p} + \left((u_{x0} + u_{x\mathrm{p}})^4\right.\\ &\qquad\left. + 2v_{\mathrm{th}x\mathrm{p}}^2v_{\mathrm{th}y0}^2 + 2v_{\mathrm{th}x\mathrm{p}}^2v_{\mathrm{th}z0}^2 + 3v_{\mathrm{th}x\mathrm{p}}^4 + 2(u_{x0} + u_{x\mathrm{p}})^2\left(3v_{\mathrm{th}x\mathrm{p}}^2 + v_{\mathrm{th}y0}^2 + v_{\mathrm{th}z0}^2\right)\right)w_\mathrm{p}\end{aligned} \tag{5}$$

with the original particle (quantities denoted by the zero subscript) split into three new particles. We assume that the middle particle, denoted subscript m, has the same drift velocity as the original particle. The two probe particles, denoted by subscript p, have drift velocities of equal magnitude but opposite sign. We now have five unknowns, the weight of the middle and probe particles, w_m and w_p, the thermal velocities of the middle and probe particles, $v_{\mathrm{th}x\mathrm{m}}$ and $v_{\mathrm{th}x\mathrm{p}}$, and the probe particle drift velocity $u_{x\mathrm{p}}$, and three equations.

If we assume some relationship between w_m and w_p we can solve for $v_{\mathrm{th}x\mathrm{m}}$ and $v_{\mathrm{th}x\mathrm{p}}$ in terms of $v_{\mathrm{th}x0}$ and $u_{x\mathrm{p}}$. There are two physically meaningful solutions for $w_\mathrm{m} = w_\mathrm{p}$

$$v_{\mathrm{th}x\mathrm{m}} = \sqrt{3v_{\mathrm{th}x0}^2 - 2\sqrt{2}u_{x\mathrm{p}}^2}\Big/\sqrt{3}, \quad v_{\mathrm{th}x\mathrm{p}} = \sqrt{3v_{\mathrm{th}x0}^2 - \left(3 - \sqrt{2}\right)u_{x\mathrm{p}}^2}\Big/\sqrt{3} \tag{6}$$

and

$$v_{\mathrm{th}x\mathrm{m}} = \sqrt{3v_{\mathrm{th}x0}^2 + 2\sqrt{2}u_{x\mathrm{p}}^2}\Big/\sqrt{3}, \quad v_{\mathrm{th}x\mathrm{p}} = \sqrt{3v_{\mathrm{th}x0}^2 - \left(3 + \sqrt{2}\right)u_{x\mathrm{p}}^2}\Big/\sqrt{3}. \tag{7}$$

For $w_\mathrm{m} = 4w_\mathrm{p}$, we again get two possible solutions:

$$v_{\mathrm{th}x\mathrm{m}} = \sqrt{3v_{\mathrm{th}x0}^2 - u_{x\mathrm{p}}^2}\Big/\sqrt{3}, \quad v_{\mathrm{th}x\mathrm{p}} = \sqrt{3v_{\mathrm{th}x0}^2 - u_{x\mathrm{p}}^2}\Big/\sqrt{3} \tag{8}$$

and

$$v_{\mathrm{th}x\mathrm{m}} = \sqrt{3v_{\mathrm{th}x0}^2 + u_{x\mathrm{p}}^2}\Big/\sqrt{3}, \quad v_{\mathrm{th}x\mathrm{p}} = \sqrt{v_{\mathrm{th}x0}^2 - 5u_{x\mathrm{p}}^2}\Big/\sqrt{3}. \tag{9}$$

These equations impose some constraints on the range of probe particle drift velocity $u_{x\mathrm{p}}$. Eq. (6) is less restrictive than Eq. (7) and requires $u_{x\mathrm{p}} < \sqrt{\frac{3}{2\sqrt{2}}}v_{\mathrm{th}x0}$. Eq. (8) is less restrictive than Eq. (9) and requires $u_{x\mathrm{p}} < \sqrt{3}v_{\mathrm{th}x0}$. If $w_\mathrm{m} = 4w_\mathrm{p}$ the middle and the two probe particles have the same thermal velocity as shown by Eq. (8).

The choice of $u_{x\mathrm{p}}$ must be made with some care as it is possible to satisfy Eqs. (3)–(5) and significantly alter the shape of the velocity distribution, as shown in Fig. 1. Very good agreement is achieved with $u_{x\mathrm{p}} = 0.5v_{\mathrm{th}x0}$, as shown in Figs. 2 and 3.

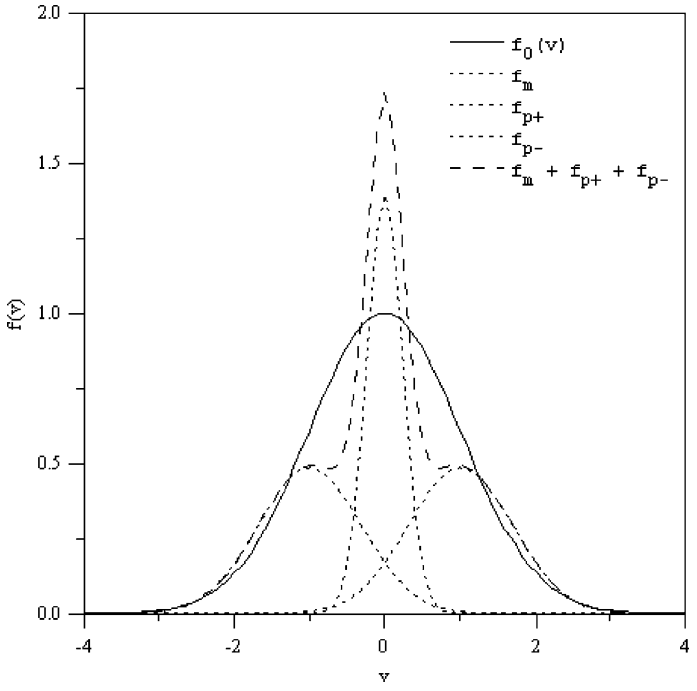

Fig. 1. Velocity distribution for $w_m = w_p$ and $u_{xp} = v_{thx0}$. At $v = 0$, $f_m + f_{p+} + f_{p-} = 1.73$.

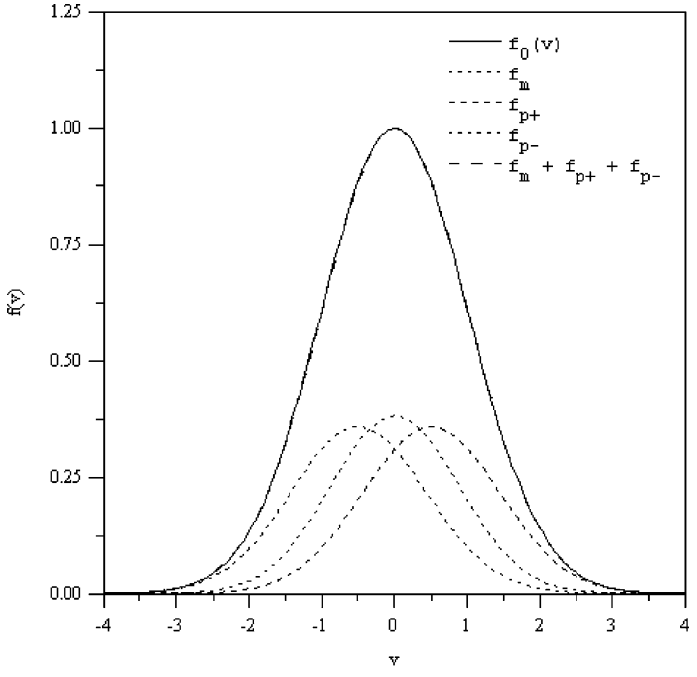

Fig. 2. Velocity distribution for $w_m = w_p$ and $u_{xp} = 0.5v_{thx0}$. At $v = 0$, $f_m + f_{p+} + f_{p-} = 1.0009$.

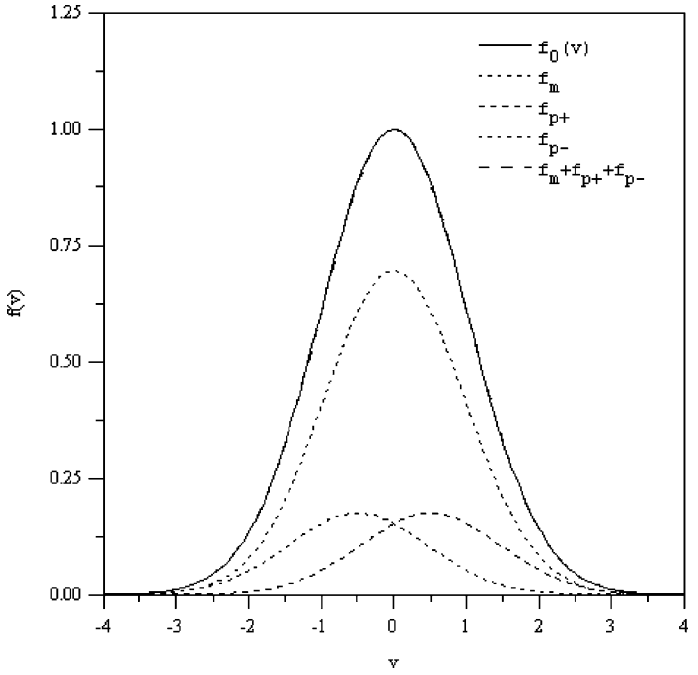

Fig. 3. Velocity distribution for $w_m = 4w_p$ and $u_{xp} = 0.5v_{thx0}$. At $v = 0$, $f_m + f_{p+} + f_{p-} = 1.00008$.

In order to reduce the number of variables carried per particle and to facilitate the particle–particle collision process, we choose to keep all particles isotropic in temperature. Thus we use the $w_m = 4w_p$ splitting with the middle and probe particle thermal velocities defined by Eq. (8). The splitting is carried out in all velocity dimensions, so one original particle becomes 27 new particles after a fully three-dimensional velocity split is complete. (Note that the middle particle can be split into four particles with weight equal to w_p, producing six particles with equal thermal velocity.) The total velocity distribution can deviate from a Maxwellian by virtue of the individual particle drift velocities.

3. Collision frequencies

The collision process between two simulation particles proceeds by equilibrating a fraction of the momentum and temperature carried by each simulation particle according to the relevant frequency for Coulomb collisions. Consider the collision force between two distinct species, α and β. As reported in [2], Decoster has performed a rigorous analysis of the fluid transport equations derived from the Boltzmann equation for two or more species. He assumes that each species consists of a drifting Maxwellian and finds two distinct collision frequencies. The fluid equations for this situation can be written as

$$n_\alpha m_\alpha \frac{\mathrm{d}}{\mathrm{d}t}\vec{v}_\alpha = -\nu_{\alpha\beta} n_\alpha m_{\alpha\beta}\left(\vec{v}_\alpha - \vec{v}_\beta\right) + \cdots, \tag{10}$$

$$\frac{3}{2} n_\alpha \frac{\mathrm{d}}{\mathrm{d}t} T_\alpha = -\nu_{\alpha\beta} n_\alpha \frac{m_{\alpha\beta}^2}{m_\alpha}\left(\vec{v}_\alpha - \vec{v}_\beta\right)\cdot\left(\vec{v}_\alpha - \vec{v}_\beta\right) - \nu_{\alpha\beta}^{\varepsilon} n_\alpha\left(T_\alpha - T_\beta\right) + \cdots, \tag{11}$$

where the $\cdots$ corresponds to the rest of the terms in the fluid equations that depend only on species α. The density, temperature, and mass of species α are n_α, T_α, and m_α. The reduced mass is $m_{\alpha\beta} = m_\alpha m_\beta/(m_\alpha + m_\beta)$. The two collision frequencies, $\nu_{\alpha\beta}$ and $\nu^{\varepsilon}_{\alpha\beta}$, are given by

$$\nu_{\alpha\beta} = \frac{8\sqrt{\pi}Z_\alpha^2 Z_\beta^2 e^4 n_\beta \ln \Lambda_{\alpha\beta}}{m_{\alpha\beta}^2 (\Delta v)^3}\left[\frac{\sqrt{\pi}}{2}\operatorname{erf}\left(\frac{\Delta v}{v_{\rm th}}\right) - \left(\frac{\Delta v}{v_{\rm th}}\right)\exp\left(-\frac{\Delta v^2}{v_{\rm th}^2}\right)\right] \tag{12}$$

and

$$\nu^{\varepsilon}_{\alpha\beta} = \frac{16\sqrt{\pi}Z_\alpha^2 Z_\beta^2 e^4 n_\beta \ln \Lambda_{\alpha\beta}}{m_\alpha m_\beta v_{\rm th}^3}\exp\left(-\frac{\Delta v^2}{v_{\rm th}^2}\right), \tag{13}$$

where $v_{\rm th}^2 \equiv 2k_{\rm B}(T_\alpha/m_\alpha + T_\beta/m_\beta)$, $\Delta v \equiv |\vec{v}_\alpha - \vec{v}_\beta|$, $\ln \Lambda_{\alpha\beta}$ is the Coulomb logarithm, and $Z_\alpha e$ is the charge of species α. Jones et al. [2] identify the frequency given by Eq. (12) with dynamic friction, while that given by Eq. (13) is related to temperature equilibration.

The dynamic friction collision frequency for $\Delta v = 0$ is found by taking the limit of Eq. (12) as $\Delta v \to 0$, which yields

$$\nu_{\alpha\beta} = \frac{16\sqrt{\pi}Z_\alpha^2 Z_\beta^2 e^4 n_\beta \ln \Lambda_{\alpha\beta}}{3m_{\alpha\beta}^2 v_{\rm th}^3}. \tag{14}$$

4. Particle–particle interactions

The macro particle–particle interactions are assumed to occur on a cell-by-cell basis. Particles residing within a cell interact, those residing in different cells do not. Each particle within a given cell is paired randomly with another particle, which may or may not be of the same species. If there are two species then each particle interacts with only one other particle in a given time step, unless an odd number of particles reside in the cell. In this case, the remaining particle is paired with another particle selected randomly from all the other particles within the cell.

If we have $N_\alpha = 100$ macro particles of species α and $N_\beta = 100$ macro particles of species β, then the total number of collision pairs is $N/2$ where $N = N_\alpha + N_\beta$. Pairing the particles randomly will yield, on average, $N_{\alpha\alpha} = 25$ interactions between α particles, $N_{\beta\beta} = 25$ interactions between β particles, and $N_{\alpha\beta} = 50$ interspecies interactions. The maximum number of $\alpha\alpha$ and $\beta\beta$ collision pairs is 50 and, of course, the maximum number of interspecies collision pairs is $N/2 = 100$. In order to correctly simulate the dynamic friction and temperature equilibration processes, we multiply the collision frequencies by the ratio of the maximum possible number of collision pairs to the average expected number of collision pairs. Thus, in this example the $\alpha\alpha$ frequencies are multiplied by a factor of 2, as are the $\beta\beta$ and $\alpha\beta$ frequencies.

Miller and Combi [4] give the following expressions for the expected number of collision pairs:

$$N_{\alpha\alpha} = \left(\frac{N}{2}\right)\frac{r_{\rm p}^2}{(1+r_{\rm p})^2},$$

$$N_{\alpha\beta} = \left(\frac{N}{2}\right)\frac{2r_{\rm p}}{(1+r_{\rm p})^2},$$

$$N_{\beta\beta} = \left(\frac{N}{2}\right)\frac{1}{(1+r_{\rm p})^2},$$

where $N = N_\alpha + N_\beta$ and $r_p = N_\alpha/N_\beta$ is the number ratio. (Note that since they are concerned with standard particle-in-cell modeling, they retain the distinction between $\alpha\beta$ and $\beta\alpha$ collisions. I have combined these in the above expressions because there is no distinction between these collisions in the algorithm under discussion.) With one modification, I use these results to determine a weighting by taking the ratio between the maximum number of pairs and the expected number. Let the maximum possible number of $\alpha\beta$ collision pairs $P_{\alpha\beta} = \min(N_\alpha, N_\beta)$ and the expected number of $\alpha\beta$ collision pairs $N_{\alpha\beta} = ((N+2)/2)(2r_p/(1+r_p)^2)$, where the addition of 2 in the numerator yields the correct weight in the limit of one particle per species. The collision frequencies are then multiplied by the following factors:

$$\begin{aligned} & & \omega_{\alpha\alpha} &= \frac{(N_\alpha/2)}{N_{\alpha\alpha}}, \\ \text{For } N_\beta \geqslant N_\alpha: & & \omega_{\alpha\beta} &= \frac{P_{\alpha\beta}}{N_{\alpha\beta}} \quad \text{and} \quad \omega_{\beta\alpha} = \frac{P_{\alpha\beta}}{N_{\alpha\beta} r_p}, \\ \text{For } N_\beta < N_\alpha: & & \omega_{\alpha\beta} &= \frac{P_{\alpha\beta}}{N_{\alpha\beta}/r_p} \quad \text{and} \quad \omega_{\beta\alpha} = \frac{P_{\alpha\beta}}{N_{\alpha\beta}}, \\ & & \omega_{\beta\beta} &= \frac{(N_\beta/2)}{N_{\beta\beta}}. \end{aligned} \tag{15}$$

The time loop is

(1) The total species density (n_α and n_β) is determined within the cell.
(2) Particles are paired randomly.
(3) $v_{\alpha\beta}$ and $v^\varepsilon_{\alpha\beta}$ are determined for each collision pair using the total species density and individual particle values for all the other quantities required.
(4) Momentum transfer between the two paired macro particles is performed and the change in thermal energy due to this process is determined.
(5) The macro particle temperatures are equilibrated taking into account the energy determined in step (4).

The momentum transfer is determined by equating the initial and final momentum of the paired simulation particles. The fraction of particle α that interacts with particle β in a time step is given by $f_\alpha = \omega_{\alpha\beta} v_{\alpha\beta} \Delta t$ and the fraction of particle β interacting with particle α is $f_\beta = \omega_{\alpha\beta} v_{\alpha\beta} (W_\alpha/W_\beta)\Delta t$, where W_α is the individual particle density. (Note that these fractions are limited to values less than or equal to one.) A new macro particle velocity is defined through the conservation of momentum

$$W_\alpha m_\alpha u_\alpha + W_\beta m_\beta u_\beta = (1-f_\alpha) W_\alpha m_\alpha u_\alpha + f_\alpha W_\alpha m_\alpha u_{\text{new}} + (1-f_\beta) W_\beta m_\beta u_\beta + f_\beta W_\beta m_\beta u_{\text{new}}$$

which yields

$$u_{\text{new}} = \frac{f_\alpha W_\alpha m_\alpha u_\alpha + f_\beta W_\beta m_\beta u_\beta}{f_\alpha W_\alpha m_\alpha + f_\beta W_\beta m_\beta}. \tag{16}$$

The change in energy due to dynamic friction, ΔE_{df}, is then given by

$$\Delta E_{\text{df}} = \frac{1}{2} W_\alpha m_\alpha (\vec{u}_\alpha - \vec{u}_{\text{new}})^2 + \frac{1}{2} W_\beta m_\beta (\vec{u}_\beta - \vec{u}_{\text{new}})^2. \tag{17}$$

Temperature equilibration is done using a similar algorithm with the fractions given by $f^\varepsilon_\alpha = \omega_{\alpha\beta} v^\varepsilon_{\alpha\beta} \Delta t$ and $f^\varepsilon_\beta = \omega_{\alpha\beta} v^\varepsilon_{\alpha\beta} (W_\alpha/W_\beta)\Delta t$. The total amount of internal energy to be equilibrated is given by

$$E_{\text{eq}} = \frac{3}{2} f^\varepsilon_\alpha W_\alpha m_\alpha v^2_\alpha + \frac{3}{2} f^\varepsilon_\beta W_\beta m_\beta v^2_\beta. \tag{18}$$

New thermal velocities are then determined

$$v^2_{\alpha\text{new}} = \frac{\frac{2}{3}(E_{\text{eq}}/2)}{f^{\varepsilon}_{\alpha} W_{\alpha} m_{\alpha}} \quad \text{and} \quad v^2_{\beta\text{new}} = \frac{\frac{2}{3}(E_{\text{eq}}/2)}{f^{\varepsilon}_{\beta} W_{\beta} m_{\beta}}$$

which are used to arrive at the final internal particle energies given by

$$\begin{aligned} E_{\alpha} &= \frac{3}{2} W_{\alpha} m_{\alpha} \left(\left(1 - f^{\varepsilon}_{\alpha}\right) v^2_{\alpha} + f^{\varepsilon}_{\alpha} v^2_{\alpha\text{new}} \right) + \frac{1}{2} \Delta E_{\text{df}}, \\ E_{\beta} &= \frac{3}{2} W_{\beta} m_{\beta} \left(\left(1 - f^{\varepsilon}_{\beta}\right) v^2_{\beta} + f^{\varepsilon}_{\beta} v^2_{\beta\text{new}} \right) + \frac{1}{2} \Delta E_{\text{df}}. \end{aligned} \tag{19}$$

New thermal velocities and temperatures are determined using these energies, keeping in mind that we require the particles to maintain isotropic internal temperatures.

As the simulation proceeds, particle pairs may emerge from the collision procedure with the same, to some specified tolerance, temperatures and velocities. These pairs can easily be merged in order to reduce the total particle count.

5. Simulation results

In this section I present the results of four homogeneous test cases and the results from a more realistic problem characteristic of laser-generated colliding plasmas. The ability to smoothly transition from the fluid limit to the fully kinetic limit is demonstrated. Rambo and Procassini [5] (hereafter referred to as R&P) used all five test cases to compare the results generated by a code using a multi-fluid algorithm with those from a fully kinetic PIC code using the Takizuka and Abe [1] collision algorithm. In general they achieved good agreement, although the PIC results reveal non-Maxwellian features of the plasma evolution, e.g., hot tails take longer to equilibrate, different parallel and perpendicular temperatures, etc. The algorithm presented above in Sections 2–4 produces results that agree with the R&P fluid code results if fragmentation is kept to a minimum and results that agree with their PIC code results if more fragmentation is employed.

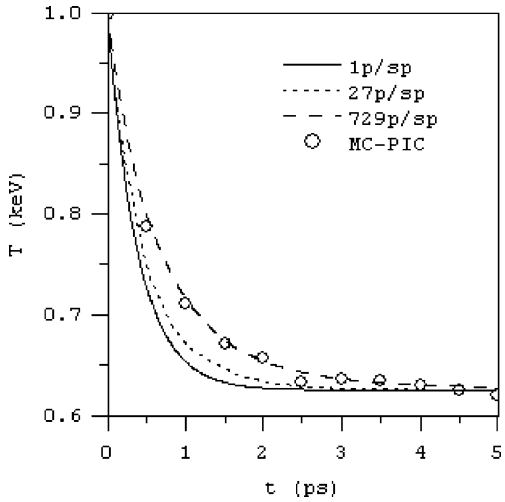

Fig. 4. Time history of T_{α} for the equal density homogeneous temperature equilibration test case.

5.1. Homogeneous tests

Two temperature equilibration simulations and two beam-slowing simulations were modeled. Each pair includes a case with equal densities and a case with a large density ratio. These tests neglect spatial gradients, ion–electron collisions, and the electric field; only the ion–ion interaction is considered. For simplicity, in all tests the Coulomb logarithm is set to $\ln \Lambda_{\alpha\beta} = 10$. As expected, using one particle per species exactly reproduces the multi-fluid results obtained by R&P for each test case. Using velocity fragmentation to generate more simulation particles produces results similar to R&P's fully kinetic results.

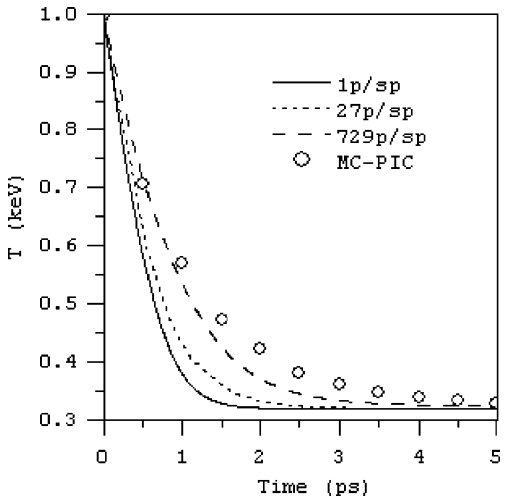

Fig. 5. Time history of T_α for the homogeneous temperature equilibration test case with unequal densities, $n_\alpha/n_\beta = 0.10$.

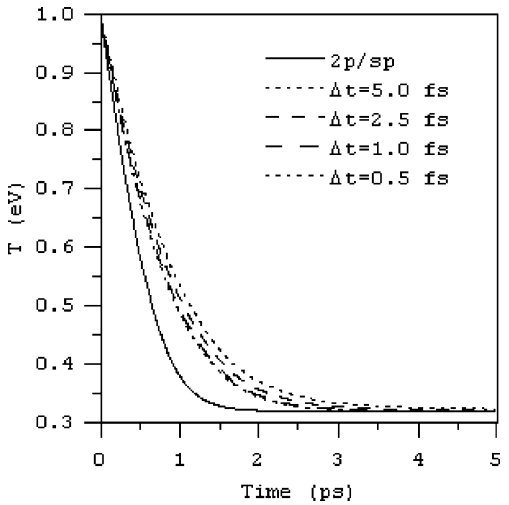

Fig. 6. Time history of the beam temperature T_α for the beam-slowing test case with equal densities. The dotted and dashed lines were obtained using two passes through the three-dimensional velocity fragmentation, producing 729 particles per species. Convergence is obtained as the time step is reduced.

The first test case consists of two Maxwellian distributions of fully ionized carbon ions, $Z = 6$ and $m = 12m_p$. With $n_\alpha = n_\beta = 1.0 \times 10^{20}$ cm^{-3}, and initial temperatures $T_\alpha = 1.0$ keV and $T_\beta = 250$ eV, the time history of the temperature of the α component is shown in Fig. 4. The solid line agrees with the multi-fluid result of R&P. The dotted line was obtained using one pass through the three-dimensional velocity fragmentation, producing 27 particles per species. The dashed line is the result obtained after two passes through the velocity fragmentation, producing 729 particles per species. The open circles are the Monte-Carlo PIC results of R&P. The plots in Figs. 5–9 use the same convention. The time step for all runs was $\Delta t = 5.0$ fs so the equilibration process is well resolved ($1/\nu^{\varepsilon}_{\alpha\beta} = 7.7 \times 10^{-13}$ s, $154\Delta t$ per relaxation time).

In the second test case the density of the hot component is reduced by a factor of 10, so $n_\alpha = 1.0 \times 10^{19}$ cm^{-3} and $n_\beta = 1.0 \times 10^{20}$ cm^{-3}. The time history of the temperature of the α component is shown in Fig. 5. The time step for all runs was again $\Delta t = 5.0$ fs.

The third and fourth test cases involve the slowing of a beam in a background plasma. We again consider fully stripped carbon ions. The third test case uses equal densities for the beam and background plasma $n_\alpha = n_\beta = 1.0 \times 10^{20}$ cm^{-3}. The beam particles are initialized with beam velocity $u_\alpha = 6.55 \times 10^7$ cm/s and temperature $T_\alpha = 500$ eV. The background plasma is initially at rest with tem-

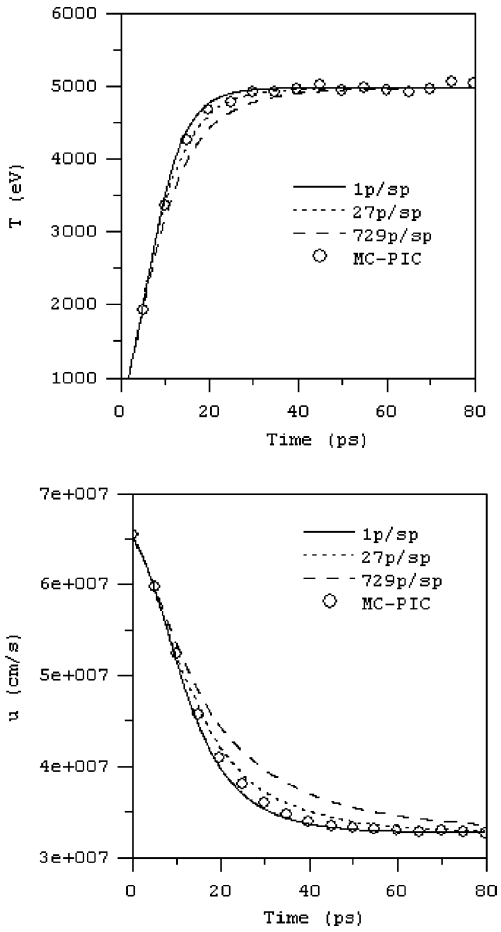

Fig. 7. Time history of T_α and the beam velocity for the equal density homogeneous beam-slowing test case.

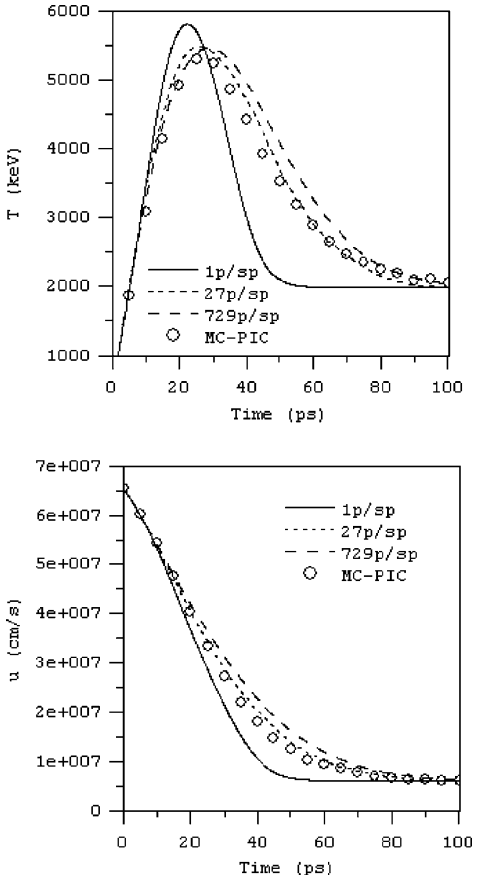

Fig. 8. Time history of T_z and the beam velocity for the unequal density beam-slowing test case.

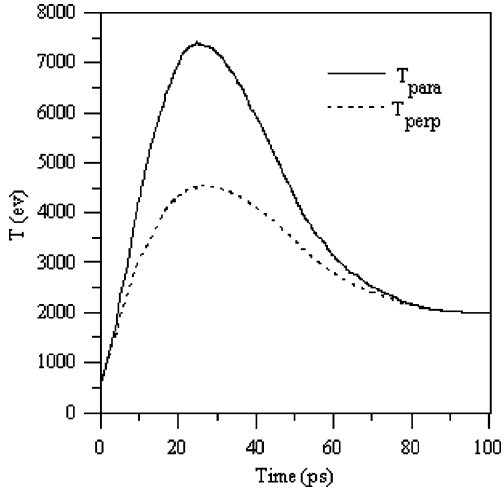

Fig. 9. Time history of the parallel and perpendicular beam temperature components for the unequal density beam-slowing test case. These results were obtained using two passes through the velocity fragmentation, producing 729 particles per species.

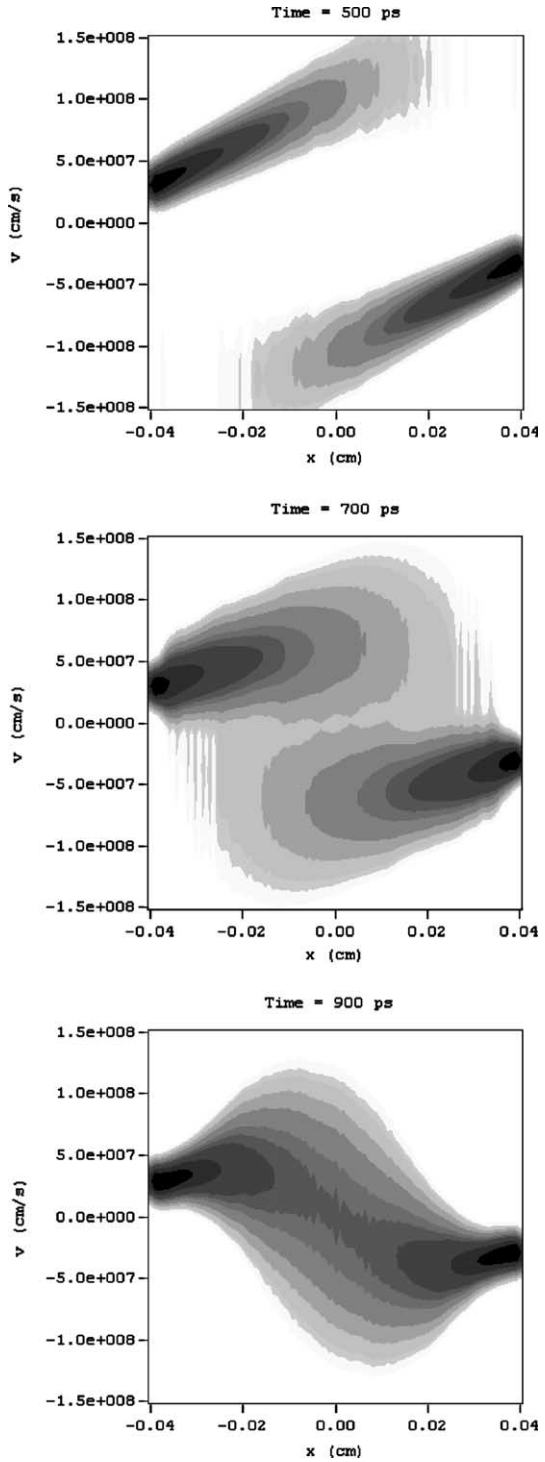

Fig. 10. Snapshots of $x - v_x$ phase space from the simulation of interpenetrating aluminum plasmas at $t = 500$, 700, and 900 ps.

perature $T_\beta = 500$ eV. Fig. 7 shows the time history of the beam velocity and the beam temperature. The time step for the third and fourth test cases was $\Delta t = 5.0$ fs.

The fourth test case incorporates unequal densities into the beam-slowing problem. We set $n_\alpha = 1.0 \times 10^{19}$ cm^{-3} and keep the other parameters unchanged from test case 3. Fig. 8 shows the time history of the beam velocity and beam temperature. The plot of parallel and perpendicular temperatures, Fig. 9, shows the deviation from a drifting Maxwellian obtained using velocity fragmentation.

The results obtained using one particle per species ran with the same time step reported by R&P [3] for their multi-fluid results, $\Delta t = 5$ fs for the temperature equilibration test cases (1 and 2) and $\Delta t = 100$ fs for the beam-slowing test cases (3 and 4). The results produced using velocity fragmentation will all converge if the time step is reduced, as shown in Fig. 6.

These results demonstrate that non-Maxwellian plasma behavior can be simulated using significantly fewer particles than would be required in the traditional Takizuka and Abe [1] approach. For instance, R&P used a total of 44,000 simulation particles to run the fourth test case. The results also illuminate the inefficiency of representing a velocity distribution using particles with discrete velocities.

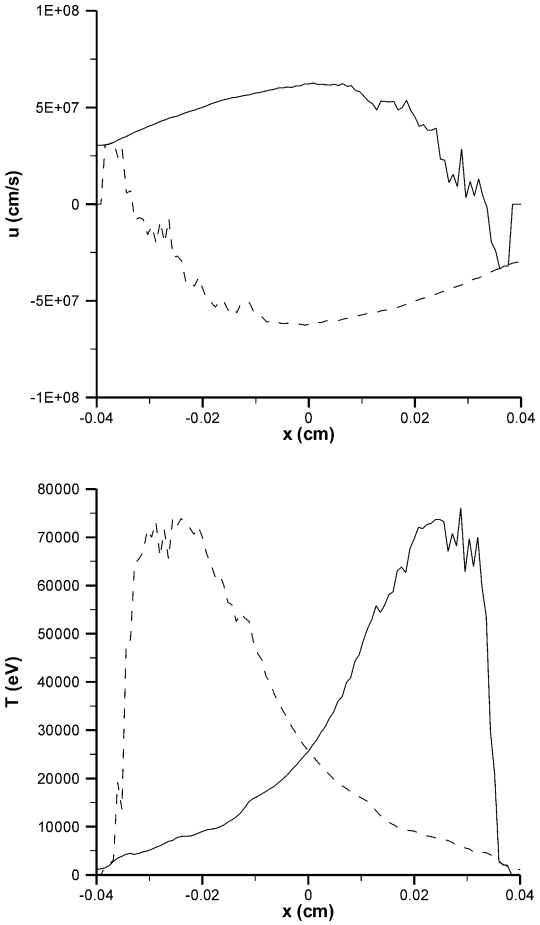

Fig. 11. Ion flow velocity and temperature from colliding aluminum plasmas at $t = 700$ ps. The solid and dashed lines indicate the two counter-streaming plasma components.

5.2. Laser-produced colliding plasma simulation

A more realistic test case involves the simulation of plasma ablated from two parallel thick discs. The problem is restricted to one spatial dimension. A code treating multiple ion species and electrons, coupled through the electric field and the Coulomb collision interaction has been written to demonstrate the potential of the velocity fragmentation procedure for modeling realistic plasmas. The electrons are assumed to be a massless fluid with density and velocity given by the quasineutrality and current-free conditions,

$$n_e \equiv \sum_i Z_i n_i \quad \text{and} \quad n_e u_e \equiv \sum_i Z_i n_i u_i, \tag{20}$$

respectively. The electric field is given by the electron momentum equation neglecting inertial effects and the magnetic field,

$$E = -\frac{1}{en_e}\frac{\partial p_e}{\partial x} - \frac{m_e}{e}\sum_i \nu_{ei}(u_e - u_i), \tag{21}$$

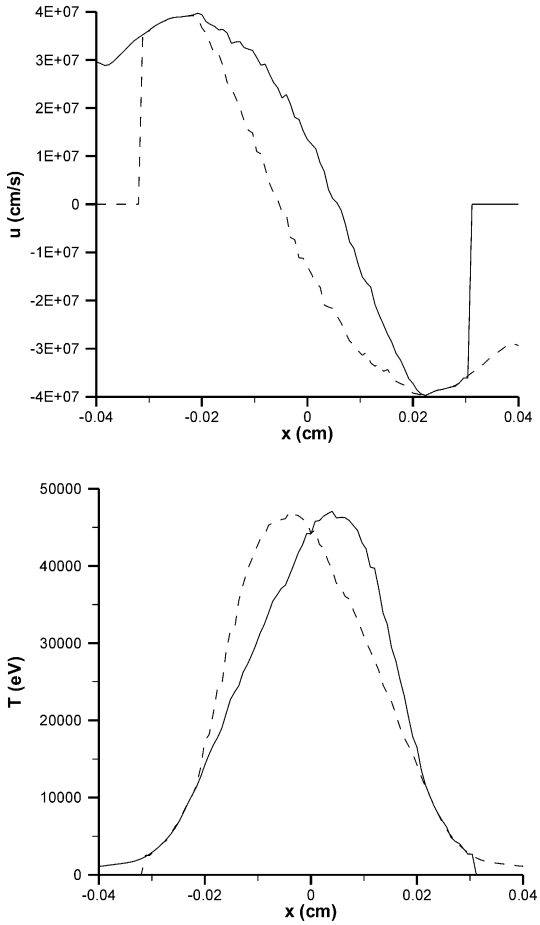

Fig. 12. Ion flow velocity and temperature from colliding aluminum plasmas at $t = 900$ ps.

where $p_e = n_e T_e$ is the electron pressure, as in [5]. The electron temperature is advanced in time by generating an electron for each ion within a cell and performing the collisional interaction for each electron–ion pair the same way the ion–ion interactions are calculated.

The problem consists of injecting identical aluminum ($A = 27, Z = 13$) plasmas on either side of an 800 μm cavity. The injection density is $n_e^0 = 2.0 \times 10^{21}$ cm^{-3}, the initial electron and ion temperatures are $T_e = 2.0$ and $T_i = 1.0$ keV, and the injection velocity is $u^0 = 3.08 \times 10^7$ cm/s. The calculation used a time step of 20 fs and a cell size of $\Delta x = 8.0$ μm. One particle was injected from each side every 70 time steps. Immediately after injection, the incoming particle was split into 27 using the velocity space fragmentation procedure. At the injection velocity a particle would cross a cell in 1300 time steps. However the particles are quickly accelerated by the electric field and the average time to cross a cell is approximately 400 time steps. The simulation ran for 900 ps. Snapshots of the phase space are shown in Fig. 10. The two beams slow and heat as the interaction proceeds, eventually equilibrating at a central temperature.

The phase space snapshots and plots of the ion drift velocity and temperature, Figs. 11 and 12, compare favorably with the fully kinetic R&P results. At $t = 900$ ps, approximately 35,000 particles are active in the simulation as compared to 90,000 particles in the R&P run. The number of particles can be drastically reduced – the algorithm recovers the multi-fluid result of R&P if velocity fragmentation is not used, producing approximately 2000 simulation particles at $t = 900$ ps. Energy conservation is excellent: the total energy injected into the simulation is $3.68156200743831 \times 10^{11}$ erg and at $t = 900$ ps the total particle energy is $3.68156203308601 \times 10^{11}$ erg, yielding an error of approximately 7×10^{-7} percent using double precision on a Pentium computer.

6. Conclusion

An algorithm for modeling partially collisional plasmas using particles that carry an isotropic thermal velocity has been presented. The method provides a smooth transition between results obtained via fluid modeling and those obtained with a fully kinetic PIC model using Monte-Carlo collisions. Results of homogeneous test problems and a 1d3v simulation of laser-produced colliding plasmas were presented. These results show that the algorithm retains non-Maxwellian plasma features, as does a fully explicit Monte-Carlo collision algorithm, but with many fewer simulation particles.

The model developed here allows the efficient simulation of partially collisional plasmas by reducing both the number of particle pairings required per time step and the number of particles needed to retain non-Maxwellian plasma behavior. The method produces reasonable results when the time step is large relative to the collision frequencies and works in the limit of one particle per species per cell. In addition, varying the amount of velocity space fragmentation smoothly links the collision-dominated and fully kinetic regimes.

Acknowledgements

The author thanks Dennis Hewett for introducing him to the concept of fragmenting a distribution function.

This work was performed under the auspices of the US Department of Energy by the University of California, Lawrence Livermore National Laboratory under Contract No. W-7405-Eng-48.

References

[1] T. Takizuka, H. Abe, J. Comp. Phys. 25 (1977) 205.
[2] M.E. Jones, D.S. Lemons, R.J. Mason, V.A. Thomas, D. Winske, J. Comp. Phys. 123 (1996) 169.

[3] P. Rambo, private communication, July 15, 1994.
[4] R.H. Miller, M.R. Combi, Geophys. Res. Lett. 21 (1994) 1735.
[5] P.W. Rambo, R.J. Procassini, Phys. Plasmas 2 (1995) 3130.
[6] D.W. Hewett, Fragmentation, merging, and internal dynamics for PIC simulation with finite size particles, J. Comp. Phys. (2003), in press.